

Simulations of Cold Electroweak Baryogenesis*

Anders Tranberg^{a†}, Jan Smit^b and Mark Hindmarsh^c

^aDAMTP, University of Cambridge,
Wilberforce Road, Cambridge CB3 0WA, United Kingdom.

^bInstitute for Theoretical Physics, University of Amsterdam,
Valckenierstraat 65, 1018XE, Amsterdam, The Netherlands.

^cDepartment of Physics and Astronomy, University of Sussex,
Brighton BN1 9QH, United Kingdom.

We present real-time lattice simulations of Cold Electroweak Baryogenesis, in which the baryon asymmetry of the Universe is generated during tachyonic electroweak symmetry breaking at the end of inflation. In the minimal realisation of the model, only three parameters remain undetermined: the strength of CP-violation, the Higgs mass and the speed of the symmetry breaking quench. The dependence of the asymmetry on these parameters is studied.

1. Cold Electroweak Baryogenesis

Baryogenesis during a zero-temperature electroweak symmetry breaking transition was proposed some time ago to bypass the lack of a first order phase transition in the Standard Model electroweak sector [1, 2, 3], (see also [4, 5, 6, 7, 8, 9, 10, 11, 12, 13, 14, 15] for related work).

Inflation is assumed to end near the electroweak scale (100 GeV), and through coupling directly to the Higgs field, the inflaton is responsible for triggering electroweak symmetry breaking. The ensuing tachyonic instability supplies departure from equilibrium, which in the presence of baryon number changing processes and CP-violation can lead to a net baryon asymmetry. It is well known that non-perturbative dynamics of the electroweak sector gauge fields may lead to baryon number (B) violation through the anomaly equation (see for instance [16])

$$B(t) - B(0) = 3\langle [N_{\text{cs}}(t) - N_{\text{cs}}(0)] \rangle = \frac{3}{16\pi^2} \int_0^t dt \int d^3\mathbf{x} \langle \text{Tr} F^{\mu\nu} \tilde{F}_{\mu\nu} \rangle, \quad (1)$$

where the Chern-Simons number N_{cs} of the $SU(2)$ gauge field is given in terms of the field strength $F^{\mu\nu}$ and its dual $\tilde{F}^{\mu\nu}$. The CP-violation in the CKM matrix of the Standard Model is likely to be much too small to account for the observed asymmetry [17, 18],

*Talk presented at Strong & Electroweak Matter (SEWM2006), BNL, United States, May 10-13, 2006.

†Speaker. A.T. is supported by PPARC SPG ‘‘Classical Lattice Field Theory’’.

and we shall here employ a generic CP-violating term, possibly originating from some extension of the SM.

Model

The simplest implementation of Cold Electroweak Baryogenesis is given through the action

$$S = - \int d^3\mathbf{x} dt \left[\frac{1}{2g^2} \text{Tr} F^{\mu\nu} F_{\mu\nu} + (D^\mu \phi)^\dagger D_\mu \phi + \mu_{\text{eff}}^2 \phi^\dagger \phi + \lambda (\phi^\dagger \phi)^2 + \kappa \phi^\dagger \phi \text{Tr} F^{\mu\nu} \tilde{F}_{\mu\nu} \right], \quad (2)$$

μ_{eff} is a time-dependent effective mass for the Higgs field. It represents the Higgs coupling to the rolling inflaton, and we will specialise to a linear form [3, 13], $\mu_{\text{eff}}^2 = [\mu^2 - \lambda_\sigma \phi \sigma^2] = \mu^2(1 - 2t/t_Q)$ where σ is the inflaton field, and we have introduced a quench time t_Q . δ_{cp} will parametrise the strength of effective CP violation through $\kappa = (3\delta_{\text{cp}})/(16\pi^2 m_W^2)$, with m_W the W mass. The Higgs self-coupling fixes the Higgs mass through $\frac{m_H}{m_W} = \sqrt{8\lambda/g^2}$.

2. Numerical results

The numerical implementation follows exactly [12] and [15]. An ensemble of initial conditions is evolved using the classical equations of motion, and the observables averaged over the ensemble. These include the Higgs expectation value $\langle \phi^\dagger \phi \rangle$, the Chern-Simons number eq. (1) and the Higgs winding number,

$$(i\tau_2 \phi^*, \phi) = \rho U, \quad U \in SU(2), \quad N_w = \frac{1}{24\pi^2} \int d^3\mathbf{x} \epsilon_{ijk} \text{Tr} \left[(\partial_i U) U^\dagger (\partial_j U) U^\dagger (\partial_k U) U^\dagger \right]. \quad (3)$$

N_w is the observable of choice since it is integer and equals the Chern-Simons number at low temperatures and therefore late times. We shall assume

$$B^{\text{final}} - B(0) = 3 \langle N_w^{\text{final}} - N_w(0) \rangle. \quad (4)$$

Dependence on m_H

In [9] and [12] we found that the mass dependence can be very strong indeed. The overall sign of the final asymmetry depends on it. Figure 1 (left) shows the final $\langle N_w \rangle$ density at $\delta_{\text{cp}} = 1$, $t_Q = 0$ for various Higgs masses. Clearly the mass dependence is non-trivial. This turns out to be a result of the conspiracy of the frequency of oscillations of the Higgs and gauge fields. For a detailed study and modelling, we refer to [15, 19]. In the following, we shall consider two specific values; $m_H = 2m_W$, $m_H = \sqrt{2}m_W$.

Dependence on t_Q

We can now vary the quench time t_Q to find figure 1 (right). For $m_H = 2m_W$, there seems to be a fast quench regime $m_H t_Q < 10$, where the asymmetry is non-zero and roughly constant. For slower quenches, the asymmetry becomes very small. Surprisingly, for $m_H = \sqrt{2}m_W$ the intermediate range of quenches gives much larger asymmetry (of the opposite sign) before decreasing to zero at very slow quenches.

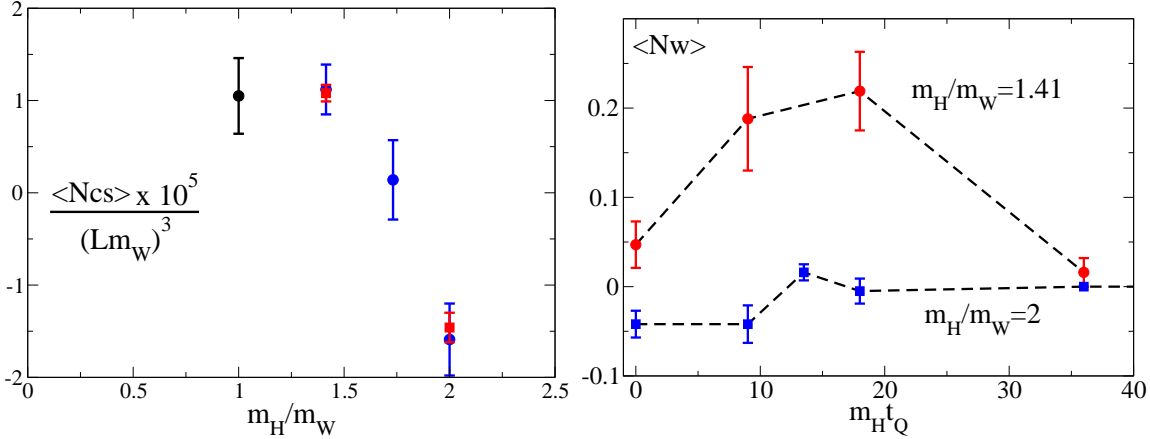


Figure 1. Left: Winding number density vs. m_H/m_W for $t_Q = 0$, $\delta_{cp} = 1$. The points with small error bars are results of linear fits to the δ_{cp} dependence (see figure 2). Right: Higgs winding number $\langle N_w \rangle$ vs. $m_H t_Q$ for $\delta_{cp} = 1$, $m_H = 2m_W$ and $m_H = \sqrt{2}m_W$.

Dependence on δ_{CP}

In figure 2 we show the dependence of $\langle N_w \rangle_{\text{final}}$ on the CP violation strength δ_{cp} for $t_Q = 0$ and $m_H = 2m_W$. In [12] we found that the dependence on δ_{cp} was non-linear for large values of δ_{cp} and we here present a zoom-in for smaller values, where the dependence is linear [15]. We will be interested in interpolating to very small values of δ_{cp} when comparing to the observed baryon asymmetry.

3. Conclusion

In order to calculate the generated baryon asymmetry in terms of the baryon (n_B) to photon (n_γ) density ratio, we use

$$\frac{n_B}{n_\gamma} = 7.04 \frac{n_B}{s}, \quad s = \frac{2\pi^2}{45} g_* T_{\text{reh}}^3, \quad \frac{\pi^2}{30} g_* T_{\text{reh}}^4 = \frac{m_H^4}{16\lambda}, \quad (5)$$

assuming that the final reheating temperature T_{reh} is given by the initial energy density, distributed over the Standard Model degrees of freedom, $g_* = 86.25$ ($T_{\text{reh}} < m_W$). With $Lm_H = 27$ and putting everything together, we for instance find for n_B/n_γ at $t_Q = 0$,

$$(0.40 \pm 0.03) \times 10^{-4} \times \delta_{cp}, \quad m_H = \sqrt{2}m_W, \quad -(0.32 \pm 0.04) \times 10^{-4} \times \delta_{cp}, \quad m_H = 2m_W.$$

The observed baryon asymmetry in the Universe $n_B/n_\gamma = 6.1 \times 10^{-10}$ [20] is reproduced for $\delta_{cp} \simeq 2 \times 10^{-5}$ for $t_Q < 10m_H^{-1}$ if the Higgs mass is around 160 GeV. In the lower end of the mass range, $m_H \simeq 120$ GeV, we can tune the quench rate to increase the asymmetry by about a factor of two. Note that this choice of Higgs mass also introduces an overall change of sign. This turns out to be the result of a conspiracy of oscillation frequencies and the complicated dynamics associated with winding and un-winding of the Higgs field. For detailed analysis of this behaviour, we refer to [15, 19].

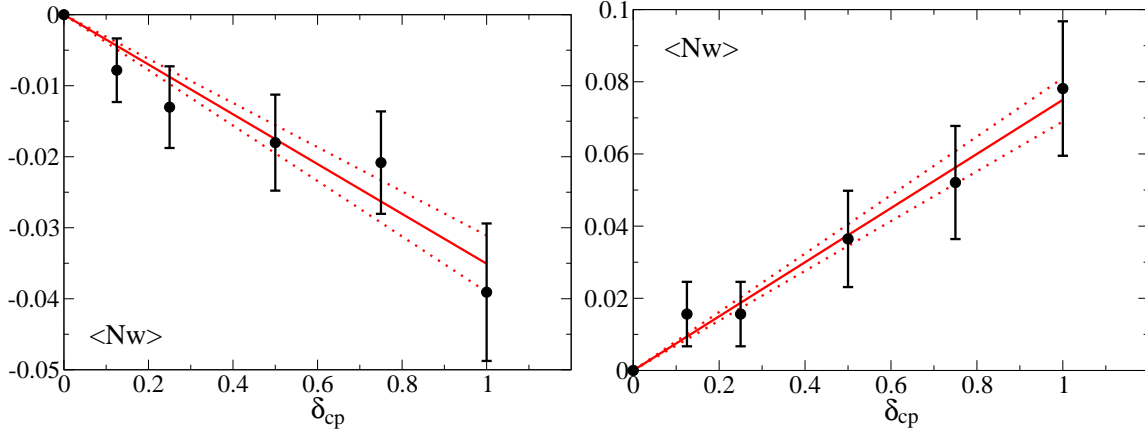


Figure 2. Higgs winding number $\langle N_w \rangle$ vs. δ_{cp} for $t_Q = 0$, $m_H = 2m_W$ (left), $m_H = \sqrt{2}m_W$ (right). Full lines are best fits, dotted lines represent 1σ in the slope. This fitted slope gives the (red/square) points of figure 1.

Acknowledgements: Part of this work was conducted on the COSMOS supercomputer funded by HEFCE, PPARC and SGI. This work received support from FOM/NWO.

REFERENCES

1. J. García-Bellido, D. Y. Grigoriev, A. Kusenko and M. E. Shaposhnikov, Phys. Rev. D **60** (1999) 123504.
2. L. M. Krauss and M. Trodden, Phys. Rev. Lett. **83** (1999) 1502.
3. E. J. Copeland, D. Lyth, A. Rajantie and M. Trodden, Phys. Rev. D **64** (2001) 043506.
4. N. Turok and J. Zadrozny, Phys. Rev. Lett. **65**, 2331 (1990).
5. N. Turok and J. Zadrozny, Nucl. Phys. B **358**, 471 (1991).
6. A. Rajantie, P. M. Saffin and E. J. Copeland, Phys. Rev. D **63** (2001) 123512.
7. E. J. Copeland, S. Pascoli and A. Rajantie, Phys. Rev. D **65** (2002) 103517.
8. J. García-Bellido, M. García Pérez and A. González-Arroyo, Phys. Rev. D **67** (2003) 103501.
9. J. Smit and A. Tranberg, JHEP **0212** (2002) 020.
10. J. I. Skullerud, J. Smit and A. Tranberg, JHEP **0308** (2003) 045.
11. J. García-Bellido, M. García-Pérez and A. González-Arroyo, Phys. Rev. D **69** (2004) 023504.
12. A. Tranberg and J. Smit, JHEP **0311** (2003) 016.
13. B. van Tent, J. Smit and A. Tranberg, JCAP **0407** (2004) 003.
14. M. van der Meulen, D. Sexty, J. Smit and A. Tranberg, JHEP **0602** (2006) 029.
15. A. Tranberg and J. Smit, JHEP **0608** (2006) 012.
16. V. A. Rubakov and M. E. Shaposhnikov, Usp. Fiz. Nauk **166**, 493 (1996).
17. M. B. Gavela, M. Lozano, J. Orloff and O. Pene, Nucl. Phys. B **430**, 345 (1994).
18. M. B. Gavela, P. Hernandez, J. Orloff, O. Pene and C. Quimbay, Nucl. Phys. B **430**, 382 (1994).

19. A. Tranberg, M. Hindmarsh and J. Smit, in preparation.
20. D. N. Spergel *et al.*, arXiv:astro-ph/0603449.